Mechanism and Machine Theory 121 (2018) 633–649

Contents lists available at ScienceDirect

Mechanism and Machine Theory

journal homepage: www.elsevier.com/locate/mechmachtheory

Research paper

Control-oriented modeling and torque estimations for vehicle driveline with dual-clutch transmission

Sooyoung Kim, Seibum Choi*

Department of Mechanical Engineering, KAIST, 291 Daehak-ro Yuseong-gu, Daejeon 307-701, Republic of Korea

ARTICLE INFO

Article history:
Received 26 July 2017
Revised 19 September 2017
Accepted 10 November 2017
Available online 6 December 2017

Keywords:
Dual clutch transmission
Control-oriented model
Clutch torque estimation
Drive shaft torque estimation
Gear shift control

ABSTRACT

Over the years, dual-clutch transmission (DCT) has demonstrated its higher efficiency and superior shift performances over other types of transmissions, and has been increasingly used in modern mass-produced vehicles. However, due to the absence of the smoothing effects of torque converters, vehicles with DCT are easily exposed to driveline oscillations that lead to poor driving quality, especially during gear shifts. Therefore, torque transfer through the driveline should be controlled with great care by two clutches and engine to achieve the DCT's outstanding performance. The main obstacle to the accurate torque control is its lack of adequate sensors in production vehicles. Thus, the objectives of this paper are two-fold. First, a control-oriented model with practical concerns is implemented for DCT drivelines, aiming to accurately describe the powertrain oscillations that should be suppressed by the torque control. Secondly, a real-time torque monitoring strategy based on the proposed model is suggested to deal with the absence of torque sensors. The primary task of the torque estimator is to concurrently estimate the torque transmitted through both clutches and drive shaft by using only readily available data from production cars. The developed torque estimator is verified through multiple experiments under various driving conditions.

1. Introduction

Dual-clutch transmissions (DCTs) use two clutches without a torque converter during gear shifts for fast and efficient torque delivery to wheels. Thus, DCTs provide a much higher fuel efficiency than conventional automatic transmissions (ATs) and also good shifting performances [1]. While shifting, DCTs allow both clutches to slip, which possibly reduces the shift duration and torque discontinuities when compared with manual transmissions (MTs) and automated manual transmissions (AMTs). Recently, after recognizing its merits, the application of DCT has expanded into pure electric vehicles as well as production hybrid electric vehicles [2–5].

For vehicles with stepped ratio transmissions such as AT, AMT, and DCT, the integrated control of the clutch(es) and engine should be performed elaborately to guarantee smooth and fast gear shifts [6]. This is especially true for a DCT where no damping effects from torque converter exists and both clutches involve gear shifts. A torque feedback control strategy can be the most effective approach to acquire a high shift performance because the basic function of the transmission system

* Corresponding author.
E-mail address: sbchoi@kaist.ac.kr (S. Choi).

https://doi.org/10.1016/j.mechmachtheory.2017.11.008
0094-114X/

is to deliver an engine torque to the wheel axle efficiently. In fact, several studies on the integrated powertrain control to improve the shift quality have explored torque-based control strategies in order to attain the shift requirements [7–12].

Since the performance of such integrated powertrain control depends heavily on the model accuracy such as those of driveline and clutch actuators, several attempts have also been made on establishing powertrain models for control. In [9], Walker et al. demonstrated the improvements of the clutch control performance for a DCT's gear shifts through the accurate modeling of the hydraulic clutch actuator. The dynamic modeling methods of a DCT driveline were investigated with an emphasis on the importance of synchronizer dynamics in [13]. Another requirement for a control-oriented model is to have a simple structure so that the controller design and implementation are affordable in real applications. Hence, a simplified driveline model of a DCT is developed in this study to precisely describe the torque fluctuations in the driveline that occur, especially during gear shifts. Considering that one main goal of the shift controller is to minimize the torque oscillations through the drive shaft that induces poor ride quality, the proposed model is suitable for designing effective torque controllers in production vehicles with DCT.

The major obstacle to the torque based powertrain control comes from the fact that torque sensors are not available on production vehicles due to their high costs and space restrictions. Previously, many studies have proposed various torque estimation methods to replace the torque sensors, particularly for vehicles with AT or AMT. Several estimation methods for turbine torque in ATs have been investigated in [14–16]. Nonlinear sliding mode observers were developed to estimate the torque through a drive shaft in [17,18], and Ibamoto et al. analyzed two different methods for estimating the drive shaft torque by using the characteristics of the engine torque map and the turbine torque map, respectively [19]. Estimation approaches using observer algorithms were proposed to estimate the drive shaft torque of AMTs in [20,21]. However, the above-mentioned estimation approaches are not appropriate for DCT because the two clutches simultaneously operate during its gear shifting and any torque converter is absent in it. Recently, some papers have reported torque estimation methods for DCT drivelines [22–24] whose applications, however, were only restricted to the vehicle launch phase in which only one clutch was involved. In [25], Zhao et al. designed a high-order sliding mode observer appropriate for estimating the torque transmitted through the two clutches during the launch with the simultaneous involvement of both clutches. Individual clutch torques during a gear shift were estimated using unscented Kalman filters in [26,27] and a Takagi–Sugeno observer in [28]. In [29,30], the authors developed novel torque estimators for a dry DCT driveline by combining multiple observers.

In fact, the estimation of torque states in the DCT during its shift transient is a quite challenging task since the torque produced by the engine can be transmitted through both clutches at the same time, which makes the estimation problem significantly more difficult than the case of one clutch systems (e.g. AMT). In this work, a novel torque observer is developed to predict the transient torque states through the DCT driveline. Though the primary role of the torque observer is to predict the drive shaft torque in real time, accurate estimation of the drive shaft torque inevitably requires individual clutch torque information. Hence, the torque observer also estimates the torque through each clutch concurrently with the drive shaft torque prediction. The information on individual clutch torques is essential for the robust actuation of the clutches in the presence of clutch wear and thermal expansion [31,32]. In addition, knowledge of the drive shaft torque can significantly improve control performances of the powertrain since the drive shaft torque is closely associated with the driving quality and the jerk as well as the vehicle acceleration. One major weakness of the previous studies is that practical studies on the concurrent monitoring of torque states through both clutches and drive shaft torque are missing. Here, the developed torque observer is characterized by its simple structure based on the aforementioned control-oriented driveline model. It also exhibits high estimation performances in spite of the presence of parametric errors such as that of the clutch friction coefficient using only the data already available in current production cars.

The rest of this paper is organized as follows. In Section 2, a control-oriented model of the DCT driveline for the accurate description of a clutch-to-clutch shift procedure is introduced. In Section 3, the torque observer is designed based on the proposed driveline model, and detailed explanations of the design procedure are also provided. In Section 4, the effectiveness of the proposed torque estimator is demonstrated through experiments under various scenarios on a DCT test-bench with torque sensors, and the results are discussed in detail. Finally, this study is concluded in Section 5.

2. Driveline model

2.1. General driveline model

Here, we discuss the modeling of the driveline part only among the powertrain components. The driveline equipped with a DCT has two sets of clutches and transfer shafts, and the torque produced by the engine is transmitted through either or both of the clutches to the wheels. The driveline model is composed of several angular speed dynamics derived by using the torque balance relationships for each component in the driveline. In this paper, the 6th order driveline model specified in [29] is used to parameterize the target DCT system. The schematic of the 6th order model is illustrated in Fig. 1. In this figure, the variables ω, θ, J, and T represent the angular speed, rotation angle, inertia, and torque, respectively.

With the assumption that the behavior of a dual-mass flywheel can be characterized as a torsional damper, (1) and (2) describe the speed dynamics of the engine and the torsional damper.

$$J_e\dot{\omega}_e = T_e - T_d, \tag{1}$$

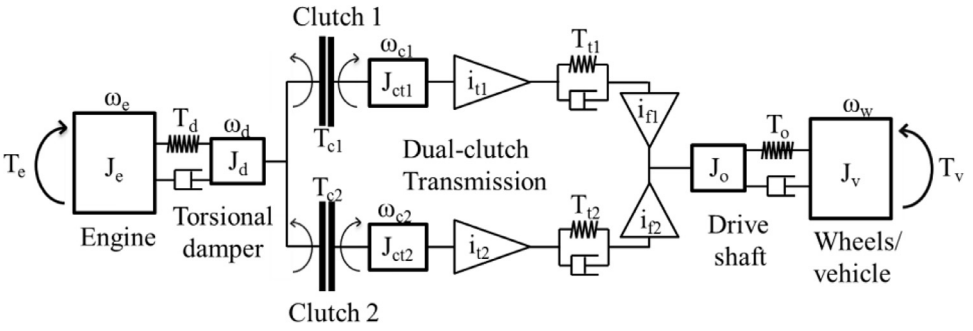

Fig. 1. DCT driveline model structure.

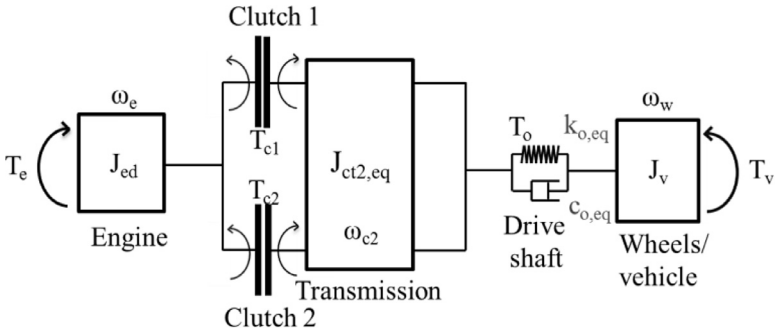

Fig. 2. Control-oriented model structure.

$$J_d\dot{\omega}_d = T_d - T_{c1} - T_{c2}, \tag{2}$$

Eq. (3) models the torque diffused through the torsional damper:

$$T_d = k_d(\theta_e - \theta_d) + c_d(\omega_e - \omega_d), \tag{3}$$

where k_d and c_d indicate the damper's torsional stiffness and damping coefficient, respectively.

After designating the components' equivalent inertias from clutches 1 and 2, including the input and transfer shafts, gears, and synchronizers, as J_{ct1} and J_{ct2}, the dynamics of each transfer shaft is described as follows:

$$J_{ct1}\dot{\omega}_{c1} = T_{c1} - \frac{T_{t1}}{i_{t1}}, \tag{4}$$

$$J_{ct2}\dot{\omega}_{c2} = T_{c2} - \frac{T_{t2}}{i_{t2}}, \tag{5}$$

where i_{t1} and i_{t2} are the gear ratios of the input and transfer shaft 1 and 2, respectively, and T_{c1}, T_{c2} the torque through each clutch, and T_{t1}, T_{t2} the torque through each transfer shaft.

Eqs. (6) and (7) indicate the torque diffused through each clutch, which depends on the clutches' status [33]:

$$T_{c1} = \begin{cases} 0 & \text{if disengaged} \\ \mu_{k1}F_{n1}r_{c1}N_1\,\mathrm{sgn}(\omega_d - \omega_{c1}) & \text{if slipping} \\ T_{in1} \triangleq T_d - T_{c2} - J_d\dot{\omega}_d, & \text{if engaged} \end{cases} \tag{6}$$

$$T_{c2} = \begin{cases} 0 & \text{if disengaged} \\ \mu_{k2}F_{n2}r_{c2}N_2\,\mathrm{sgn}(\omega_d - \omega_{c2}) & \text{if slipping} \\ T_{in2} \triangleq T_d - T_{c1} - J_d\dot{\omega}_d, & \text{if engaged} \end{cases} \tag{7}$$

where μ_k, F_n, r_c and N represent the kinetic coefficient, actuator normal force, effective torque radius, and number of friction surfaces of each clutch, respectively.

The dynamics of the drive shaft and wheel are derived as (8)-(9) after the principle of the torque balance is used.

$$J_o\dot{\omega}_o = i_{f1}T_{t1} + i_{f2}T_{t2} - T_o, \tag{8}$$

$$J_v\dot{\omega}_w = T_o - T_v, \tag{9}$$

where T_o represents the torque for the drive shaft, while T_v indicates the torque for the vehicle load.

From using the torsional compliance model, the drive shaft torque can be expressed as (10).

$$T_o = k_o(\theta_o - \theta_w) + c_o(\omega_o - \omega_w), \tag{10}$$

where k_o and c_o are the torsional stiffness and damping coefficient of the drive shaft, respectively.

The load torque influenced by the road's inclination, aerodynamic drag, and rolling resistance can be calculated by (11):

$$T_v = \left(M_v g \sin(\varphi) + \frac{1}{2}\rho_{air}A_v C_D V^2 + M_v g C_{rr}\right) r_w. \tag{11}$$

In (11), M_v, φ, ρ_{air}, A_v, C_D, V, C_{rr} and r_w indicate the vehicle's mass, angle of road inclination, air density, vehicle frontal area, drag coefficient, vehicle speed, rolling resistance coefficient, and wheel radius.

2.2. Control-oriented model

2.2.1. Design procedure

In order to be adopted for automotive control applications, the driveline model needs to be further simplified. Considering the gear shift of the DCT is performed through the torque handover from one clutch to the other clutch in the driveline, i.e. a clutch-to-clutch shift, a reduced driveline model should be implemented that focuses on the clutch-to-clutch shift procedure. Another structural requirement of the control-oriented model is that the model should describe the behavior of the driveline system as accurately as possible by using already available information in production cars. The model should also be simple enough to be used for control purposes.

First, we define the new three states x_1, x_2, x_3 as follows:

$$\begin{aligned} x_1 &\triangleq \omega_e - \omega_{c2}, \\ x_2 &\triangleq \tfrac{\omega_{c2}}{i_{t2}i_{f2}} - \omega_w, \\ x_3 &\triangleq T_o. \end{aligned} \tag{12}$$

Here, x_1 stands for the slip speed between the engine and the oncoming clutch (clutch 2), while x_2 describes the torsional compliance rate through the shafts. In general, x_1 and x_3 are considered as control outputs of a shift control system, since the control performance of those states determines the shift quality. Assuming the compliances through the torsional damper, input shafts, and transfer shafts can be neglected, i.e., $\omega_e \approx \omega_d$ and $\omega_o \approx \frac{\omega_{c2}}{i_{t2}i_{f2}}$ so that immeasurable states are eliminated from the model, the time derivative of x_1 is described as (13) by combining (1), (2), (4), (5), and (8).

$$\begin{aligned} \dot{x}_1 &= \frac{1}{J_{ct2,eq}}x_3 + \frac{1}{J_{ed}}T_e - \left(\frac{1}{J_{ed}} + \frac{i_{t2}i_{f2}}{J_{ct2,eq}}\right)T_{c2} - \left(\frac{1}{J_{ed}} + \frac{i_{t1}i_{f1}}{J_{ct2,eq}}\right)T_{c1} \\ &\text{where } J_{ed} = J_e + J_d, \\ J_{ct2\_eq} &= \left(i_{t2}i_{f2}J_{ct2} + \frac{(i_{t1}i_{f1})^2}{i_{t2}i_{f2}}J_{ct1} + \frac{1}{i_{t2}i_{f2}}J_o\right). \end{aligned} \tag{13}$$

In (13), J_{ct2_eq} is the equivalent inertia seen from the on-coming clutch that includes the inertias of all the components rotating synchronously with the input shaft 2.

Likewise, the dynamics of x_2 is easily derived as (14).

$$\dot{x}_2 = -\left(\frac{1}{i_{t2}i_{f2}J_{ct2,eq}} + \frac{1}{J_v}\right)x_3 + \frac{i_{t1}i_{f1}}{i_{t2}i_{f2}J_{ct2,eq}}T_{c1} + \frac{1}{J_{ct2,eq}}T_{c2} + \frac{1}{J_v}T_v. \tag{14}$$

The state x_2 provides valuable information to predict the transient behavior of the driveline. It is worth noting that x_2 can be easily measured on the production DCTs. In [34], the author tried to suppress the driveline oscillations in a production dry DCT through implementing a torque controller based on the measurements of x_2.

The dynamics of the drive shaft torque x_3 is obtained using (14) with both the stiffness and damping coefficients remaining in it, as follows:

$$\begin{aligned} \dot{x}_3 &= k_{o,eq}x_2 + c_{o,eq}\dot{x}_2 \\ &= k_{o,eq}x_2 - c_{o,eq}\left(\frac{1}{i_{t2}i_{f2}J_{ct2,eq}} + \frac{1}{J_v}\right)x_3 + c_{o,eq}\left(\frac{i_{t1}i_{f1}}{i_{t2}i_{f2}J_{ct2,eq}}T_{c1} + \frac{1}{J_{ct2,eq}}T_{c2}\right) + \frac{c_{o,eq}}{J_v}T_v, \end{aligned} \tag{15}$$

where $k_{o,\,eq}$ and $c_{o,\,eq}$ are the equivalent torsional stiffness and damping coefficients of the drive shaft in the reduced order model. It should be emphasized that previously, the damping coefficient of the driveline shaft was often removed from the control-oriented powertrain models for simplicity. That is mainly because using both the stiffness and damping parameters

requires the inclusion of an additional state of torsional angle in the model. In fact, in some relevant studies, the stiffness and damping behavior of the shaft was modeled based on the information of its torsional angle as well as its compliance rate. However, using the torsional angle data is not desirable because the data should be indirectly acquired by integrating the angular speed with unavoidable measurement noise [35]. Hence, in order to deal with the aforementioned problems effectively, a model structure (13)–(15) was developed so that the torsional damping characteristics of the drive shaft were also described without increasing the number of states. Finally, the control-oriented model (13)–(15) can be represented as a standard linear control system, as follows:

$$\begin{aligned}
&\dot{\mathbf{x}} = \mathbf{A}\mathbf{x} + \mathbf{B}\mathbf{u} + \mathbf{E}\delta \\
&\mathbf{x} = (x_1,\ x_2,\ x_3),\ \ \mathbf{u} = (T_e,\ T_{c1},\ T_{c2}),\ \ \delta = T_v \\
&\mathrm{A} = \begin{bmatrix} 0 & 0 & \frac{1}{J_{ct2,eq}} \\ 0 & 0 & -\left(\frac{1}{i_{t2}i_{f2}J_{ct2,eq}} + \frac{1}{J_v}\right) \\ 0 & k_{o,eq} & -c_{o,eq}\left(\frac{1}{i_{t2}i_{f2}J_{ct2,eq}} + \frac{1}{J_v}\right) \end{bmatrix}, \\
&\mathbf{B} = \begin{bmatrix} \frac{1}{J_{ed}} & -\left(\frac{1}{J_{ed}} + \frac{i_{t1}i_{f1}}{J_{ct2,eq}}\right) & -\left(\frac{1}{J_{ed}} + \frac{i_{t2}i_{f2}}{J_{ct2,eq}}\right) \\ 0 & \frac{i_{t1}i_{f1}}{i_{t2}i_{f2}J_{ct2,eq}} & \frac{1}{J_{ct2,eq}} \\ 0 & \frac{c_{o,eq}i_{t1}i_{f1}}{i_{t2}i_{f2}J_{ct2,eq}} & \frac{c_{o,eq}}{J_{ct2,eq}} \end{bmatrix},\ \ \mathbf{E} = \begin{bmatrix} 0 \\ \frac{1}{J_v} \\ \frac{c_{o,eq}}{J_v} \end{bmatrix}.
\end{aligned} \tag{16}$$

2.2.2. Identification of model parameters

One important assumption for the model development (16) is that the drive shaft is regarded as a linear torsional spring-damper, whose torsional compliance is captured by the angular speed difference between the clutch 2 (divided by gear ratios) and the wheel axle. Accurate identification of the equivalent coefficients, $k_{o,\,eq}$ and $c_{o,\,eq}$ is an essential task in the model development since the coefficients exclusively determine the transient behavior of the modeled driveline. Denoting angular positions of the input shaft with clutch 2 and the wheel axle as θ_{c2} and θ_w, the drive shaft torque is explicitly represented as (17) suitable for the parameter identification:

$$\begin{aligned}
&T_o = X\beta, \\
&\text{where } X = \begin{bmatrix} \frac{\theta_{c2}}{i_{t2}i_{f2}} - \theta_w & \frac{\omega_{c2}}{i_{t2}i_{f2}} - \omega_w \end{bmatrix},\ \ \beta = \begin{bmatrix} k_{o,eq} \\ c_{o,eq} \end{bmatrix}.
\end{aligned} \tag{17}$$

In order to analyze the relation between the drive shaft torque and the torsional compliance, some experimental data on the torsional angular velocity (x_2)/angle of drive shaft are exhibited in Fig. 3.

The data were obtained by the experiments on a test-bench of a dry-type DCT under the driving scenario of vehicle launch and a gear shift from 1st to 2nd gear. Note that the angular position data was indirectly obtained by integrating the measured angular speed with respect to time. Because the angular speed data always accompanies measurement noise, the corresponding angle data calculated by time integration of it is not reliable, especially as the integration time increases. Also, it is deduced from (17) that if the torsional angular velocity/angle are close to zero while the drive shaft torque is still positive, the accuracy of the identified coefficients would be highly sensitive to the measurement errors. Hence, to avoid the aforementioned problems, only the part (marked in Fig. 3) of the measured data is used for the parameter identification. The data of interest corresponds to the initial part of vehicle launching.

Then, the least square solution to (17) can be obtained by (18).

$$\hat{\beta} = \begin{bmatrix} \hat{k}_{o,eq} \\ \hat{c}_{o,eq} \end{bmatrix} = \left(X^T X\right)^{-1} X^T T_o. \tag{18}$$

The corresponding identified parameter values are as follows: $\hat{k}_{o,eq} = 4887,\ \hat{c}_{o,eq} = 561$.

It is worth noting that the parameter values were identified using the data obtained only after the output torque was generated to avoid initial calculation errors caused by backlash between gears. The identified damping coefficient indicates the damping characteristics of mechanical components mounted between the clutches and the axle shaft, such as the frictional losses, as well as that of the drive shaft itself.

2.2.3. Model validation

To evaluate the accuracy of the proposed control-oriented model, experiments were conducted on a DCT test-bench. The mechanical structure of the DCT was exactly the same as the ones produced, but several torque/speed sensors were additionally attached on the shafts for validation purposes. The detailed information on the test-bench set-ups is provided in Section 4.

Since we focused on the accuracy of the driveline dynamics only, torque inputs were directly applied to obtain the model responses so that the influences of the clutch actuator dynamics, including the actuator delay and variations of the friction

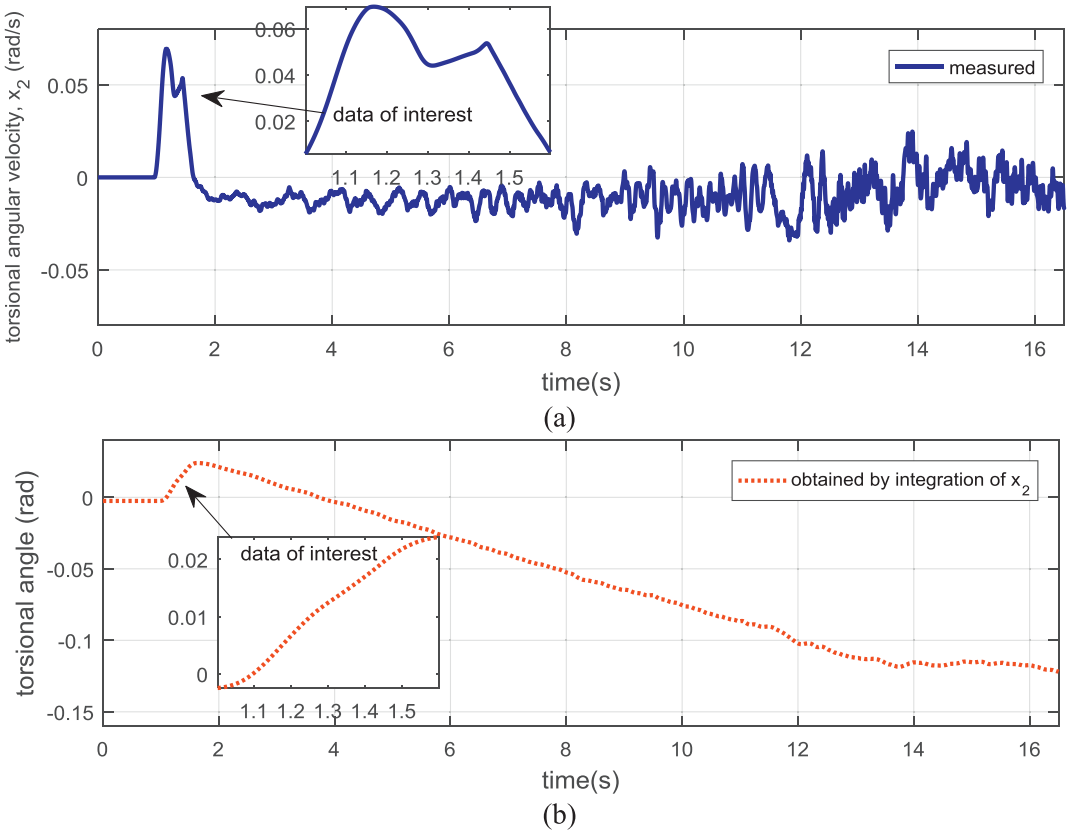

Fig. 3. Data for parameter identification: (a) torsional angular velocity of the transmission, x_2 (b) torsional angle of the transmission.

coefficient on the driveline model response, were eliminated. Fig. 5 exhibits the responses of the proposed model and the actual DCT corresponding to the test conditions described in Fig. 4. The test conditions involved a vehicle launch and an upshift from 1st to 2nd gear. Note that Fig. 5 also exhibited the response of the model without the damping parameter in order to demonstrate the effectiveness of the proposed model.

In Fig. 5(a), the inaccuracy of the lumped inertias (e.g. J_{ed}, $J_{ct2,\,eq}$) produced the errors in the slip speed responses of both models, especially during the launch phase. However, the conventional model (without the damping term) exhibited much larger errors in the transient responses of the drive shaft torque (Fig. 5(b)) when compared with the proposed one. Even though the conventional model described the oscillations through the drive shaft reasonably in some driving conditions (e.g., 2∼5 s in Fig. 5(b)), the model did not cover all of the test conditions, including the gear shifting phase (13∼16 s in (Fig. 5(b)), particularly when a non-variable stiffness value was used. Because the damping term was not included in the conventional model, it exhibited little attenuated oscillatory responses, and unable to describe the natural damping characteristics of the transmission system such as the frictional losses. On the other hand, the proposed model predicted the responses of the actual driveline well throughout the test conditions.

3. Driveline torque estimation

3.1. Overview

A common objective of the clutch-to-clutch shift control is to minimize the torque oscillations through the drive shaft and the shift duration simultaneously [7,11]. Since such control requirements are directly associated with torque states in the driveline, a lot of research has been done on the torque-based control approach to improve shift quality. However, the main problem arising in the controller implementation is that driveline torque states such as the torque through the drive shaft cannot be measured on production vehicles. The drive shaft torque determines the quality of the ride and the acceleration characteristics of a vehicle, so knowledge of this drive shaft possibly enhances not only the performances of powertrain control, but also those of longitudinal dynamics control. Hence, the main purpose of this section is to introduce a novel torque estimation approach for vehicle drivelines equipped with a DCT. The design procedure of the torque estimator will be presented in the following sub-section.

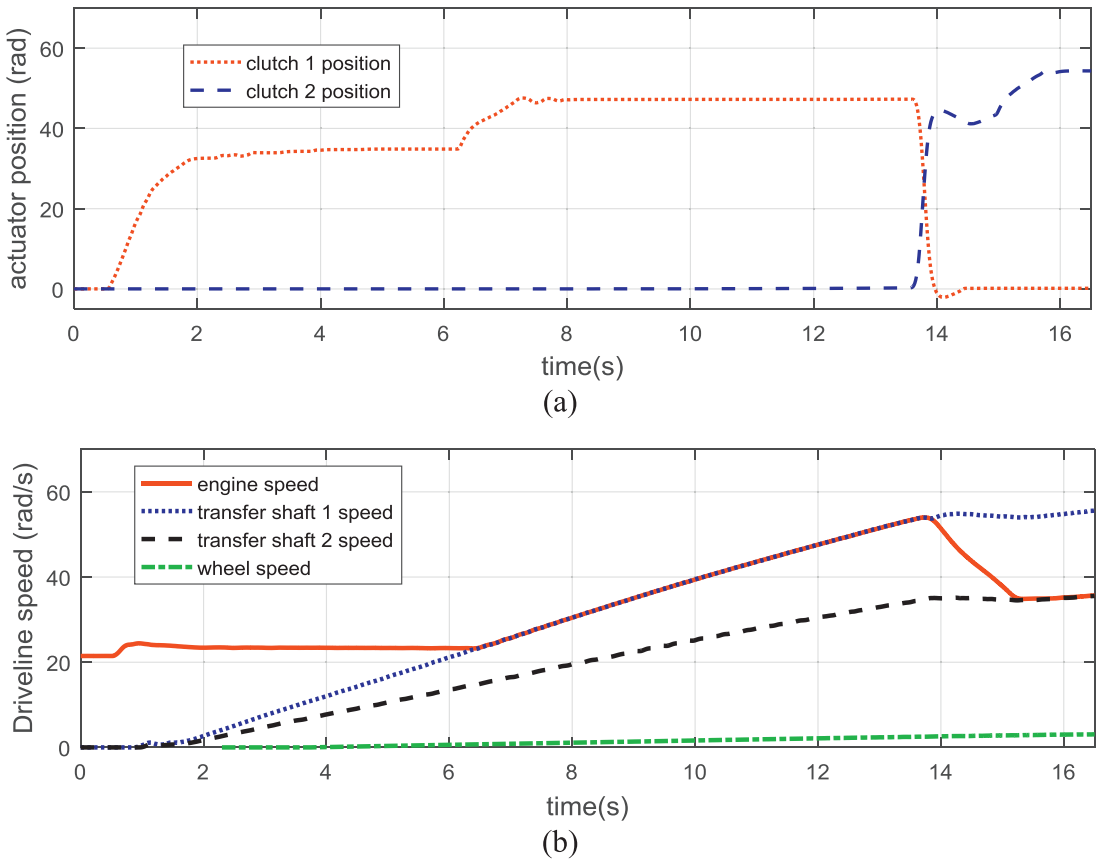

Fig. 4. Conditions for model validation: (a) clutch position, (b) driveline speed.

3.2. Torque observer design

First, using (16), a Luenberger state observer is developed to estimate the drive shaft torque, as follows:

$$\begin{aligned}&\dot{\hat{\mathbf{x}}} = \mathbf{A}\hat{\mathbf{x}} + \mathbf{B}\hat{\mathbf{u}} + \mathbf{E}\delta + \mathbf{LC}\tilde{\mathbf{x}}\\ &\text{where } \hat{\mathbf{x}} = \left(\hat{x}_1,\ \hat{x}_2,\ \hat{x}_3\right),\ \hat{\mathbf{u}} = \left(T_e,\ \hat{T}_{c1},\ \hat{T}_{c2}\right),\ \delta = T_v\\ &\mathbf{C} = \begin{bmatrix}1 & 0 & 0\\ 0 & 1 & 0\end{bmatrix},\ \mathbf{L} = \begin{bmatrix}L_{11} & L_{12}\\ L_{21} & L_{22}\\ L_{31} & L_{32}\end{bmatrix}.\end{aligned} \tag{19}$$

Here, **L** is the observer gain matrix to be designed later.

The vehicle load torque can be calculated by using (11) with $V \approx r_w\omega_w$, but the calculated load value is inevitably inaccurate due to large parametric errors of (11). Instead, we can obtain the relatively accurate load value by combining the engine torque multiplied by gear ratios and the whole vehicle inertia, as follows:

$$T_v = i_t i_f T_e - J_{v,eq}\dot{\omega}_w, \tag{20}$$

where i_t, i_f is the current gear ratio and $J_{v,\,eq}$ is the equivalent vehicle inertia from wheel perspective when one of the clutches is engaged with the flywheel.

Note that the Eq. (20) is valid only when one of the clutches is fully engaged and the other clutch one is disengaged. Thus, (20) is applicable to most driving conditions except for the short durations of gear shifts and vehicle launch. Under the assumption that the vehicle load does not change during the short time of the vehicle launch and each gear shift, (20) is used alternatively to (11) in the torque observer design.

Another serious difficulty in the state estimation using (19) arises from the inaccurate information of the input values **u**, particularly that of the clutch torques, i.e. T_{c1}, T_{c2}. Thus, the ultimate task of the developed torque observer is to conduct simultaneous estimation of the transient torque through both clutches and the drive shaft.

Based on (6)-(7), the clutch torque model valid for the slipping phase is rearranged as (21) and (22) to remove the normal force terms.

$$T_{c1} = \mu_{k1} r_{c1} N_1 F_{n1} = \mu_{k1} r_{c1} N_1 f_1 \theta_{m1}. \tag{21}$$

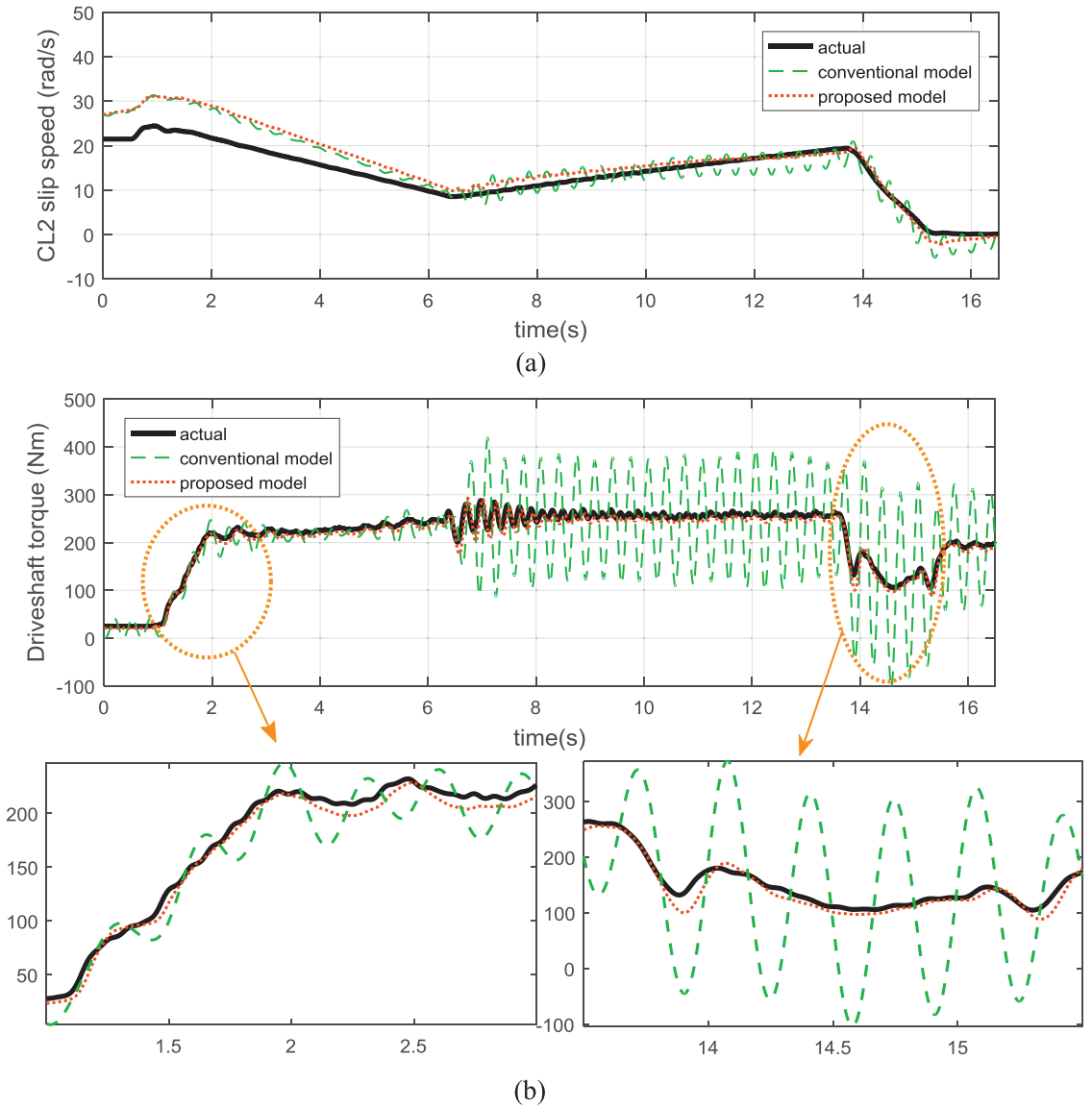

Fig. 5. Model validation: (a) slip speed of the on-coming clutch, x_1 (b) drive shaft torque, x_3 Conventional model means the model without damping coefficient.

$$T_{c2} = \mu_{k2} r_{c2} N_2 F_{n2} = \mu_{k2} r_{c2} N_2 f_2 \theta_{m2}. \tag{22}$$

In (21) and (22), the normal forces F_{n1}, F_{n2}, which cannot be directly measured, are replaced with the actuator positions θ_{m1}, θ_{m2} multiplied by some force coefficients f_1, f_2. The force coefficients f_1, f_2 can be identified by experiments on the clutch actuator module, generally in the form of a look-up table, one example of which is described in Fig. 6. However, both the dynamic friction coefficient and force coefficient change continuously based on the slip rate of the clutch and other environmental factors such as temperature [31,36]. When the nominal values of the friction coefficient and force coefficient, denoted as $\mu_{k1,n}$, $\mu_{k2,n}$, f_{1n}, f_{2n}, are known, the Eqs. (21) and (22) can be modified as follows:

$$T_{c1} = \left(\mu_{k1,n} f_{1,n} + \varepsilon_{c1}\right) r_{c1} N_1 \theta_{m1}, \tag{23}$$

$$T_{c2} = \left(\mu_{k2,n} f_{2,n} + \varepsilon_{c2}\right) r_{c2} N_2 \theta_{m2}, \tag{24}$$

where ε_{c1}, ε_{c2} stand for the uncertain parts of the clutch parameters.

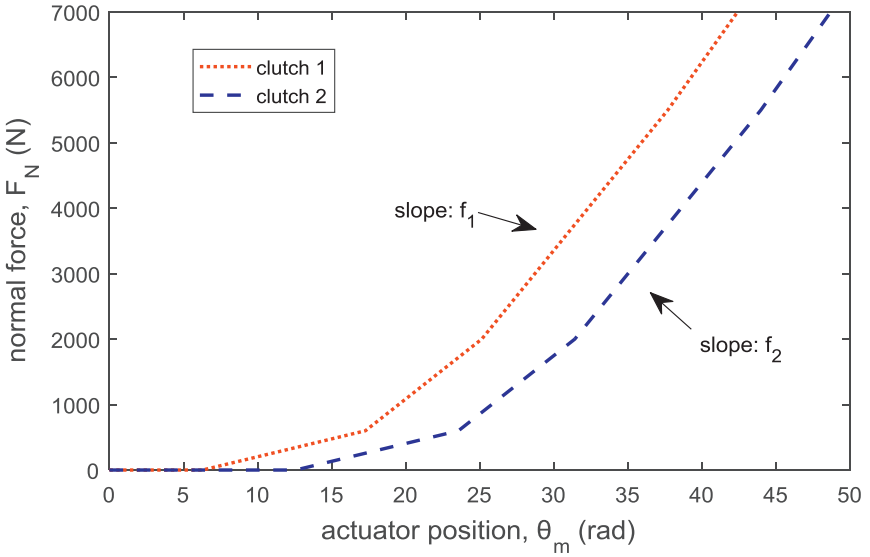

Fig. 6. Force-position map for clutches (dry-type).

In order to design proper adaptation laws to treat the parametric uncertainties, a Lyapunov function candidate, which is positive definite and radially unbounded, is chosen as follows:

$$\begin{aligned}&\dot{V} = \tfrac{1}{2}\tilde{x}_1^2 + \tfrac{1}{2}\tilde{x}_2^2 + \tfrac{1}{2}(c_{o,eq}\tilde{x}_2 - \tilde{x}_3)^2 + \tfrac{1}{2L_{c1}}\tilde{\varepsilon}_{c1}^2 + \tfrac{1}{2L_{c2}}\tilde{\varepsilon}_{c2}^2,\\ &\text{where } \tilde{x}_1 \triangleq x_1 - \hat{x}_1,\ \tilde{x}_2 \triangleq x_2 - \hat{x}_2,\ \tilde{x}_3 \triangleq x_3 - \hat{x}_3,\\ &\tilde{\varepsilon}_{c1} \triangleq \varepsilon_{c1} - \hat{\varepsilon}_{c1},\ \ \tilde{\varepsilon}_{c2} \triangleq \varepsilon_{c2} - \hat{\varepsilon}_{c2}.\end{aligned} \tag{25}$$

In (25), $\hat{\varepsilon}_{c1}$, $\hat{\varepsilon}_{c2}$ are the parameters estimated through the adaptations and $L_{c1}, L_{c2} > 0$ are the adaptation gains to be designed.

Under the assumption that variations of the clutch parametric uncertainties are slow, i.e., $\dot{\varepsilon}_{c1},\ \dot{\varepsilon}_{c2} \approx 0$, the time derivative of (25) is derived as (26) by substituting (16) and (19) into it.

$$\begin{aligned}\dot{V} &= \tilde{x}_1\dot{\tilde{x}}_1 + \left(c_{o,eq}^2 + 1\right)\tilde{x}_2\dot{\tilde{x}}_2 + \tilde{x}_3\dot{\tilde{x}}_3 - c_{o,eq}\tilde{x}_3\dot{\tilde{x}}_2 - c_{o,eq}\tilde{x}_2\dot{\tilde{x}}_3 - \frac{1}{L_{c1}}\tilde{\varepsilon}_{c1}\dot{\hat{\varepsilon}}_{c1} - \frac{1}{L_{c2}}\tilde{\varepsilon}_{c2}\dot{\hat{\varepsilon}}_{c2}\\ &= \tilde{x}_1\left(\frac{1}{J_{ct2,eq}}\tilde{x}_3 - \left(\frac{1}{J_{ed}} + \frac{i_{t2}i_{f2}}{J_{ct2,eq}}\right)r_{c2}N_2\theta_{m2}\tilde{\varepsilon}_{c2} - \left(\frac{1}{J_{ed}} + \frac{i_{t1}i_{f1}}{J_{ct2,eq}}\right)r_{c1}N_1\theta_{m1}\tilde{\varepsilon}_{c1} - L_{11}\tilde{x}_1 - L_{12}\tilde{x}_2\right)\\ &\quad + \left(c_{o,eq}^2 + 1\right)\tilde{x}_2\left(-\left(\frac{1}{i_{t2}i_{f2}J_{ct2,eq}} + \frac{1}{J_v}\right)\tilde{x}_3 + \frac{i_{t1}i_{f1}}{i_{t2}i_{f2}J_{ct2,eq}}r_{c1}N_1\theta_{m1}\tilde{\varepsilon}_{c1} + \frac{1}{J_{ct2,eq}}r_{c2}N_2\theta_{m2}\tilde{\varepsilon}_{c2} - L_{21}\tilde{x}_1 - L_{22}\tilde{x}_2\right)\\ &\quad + \tilde{x}_3\left(k_{o,eq}\tilde{x}_2 + c_{o,eq}\dot{\tilde{x}}_2 - L_{31}\tilde{x}_1 - L_{32}\tilde{x}_2\right) - c_{o,eq}\dot{\tilde{x}}_2\tilde{x}_3 - c_{o,eq}\left(k_{o,eq}\tilde{x}_2 - c_{o,eq}\left(\frac{1}{i_{t2}i_{f2}J_{ct2,eq}} + \frac{1}{J_v}\right)\tilde{x}_3\right.\\ &\quad \left. + c_{o,eq}\left(\frac{i_{t1}i_{f1}}{i_{t2}i_{f2}J_{ct2,eq}}r_{c1}N_1\theta_{m1}\tilde{\varepsilon}_{c1} + \frac{1}{J_{ct2,eq}}r_{c2}N_2\theta_{m2}\tilde{\varepsilon}_{c2}\right) - L_{31}\tilde{x}_1 - L_{32}\tilde{x}_2\right)\tilde{x}_2 - \frac{1}{L_{c1}}\tilde{\varepsilon}_{c1}\dot{\hat{\varepsilon}}_{c1} - \frac{1}{L_{c2}}\tilde{\varepsilon}_{c2}\dot{\hat{\varepsilon}}_{c2}.\end{aligned} \tag{26}$$

If the observer gains are set to satisfy the following requirements,

$$L_{11} > 0,\ \ L_{12} \triangleq \frac{c_{o,eq}}{J_{ct2,eq}},\ L_{21} \triangleq 0,\ L_{22} > \frac{c_{o,eq}}{\left(c_{o,eq}^2 + 1\right)}\left(\frac{1}{i_{t2}i_{f2}J_{ct2,eq}} + \frac{1}{J_v}\right),\ L_{31} \triangleq \frac{1}{J_{ct2,eq}},\ L_{32} \triangleq k_{o,eq} - \left(\frac{1}{i_{t2}i_{f2}J_{ct2,eq}} + \frac{1}{J_v}\right), \tag{27}$$

the Eq. (26) is reduced to (28) after cancelling the multiple terms one after another.

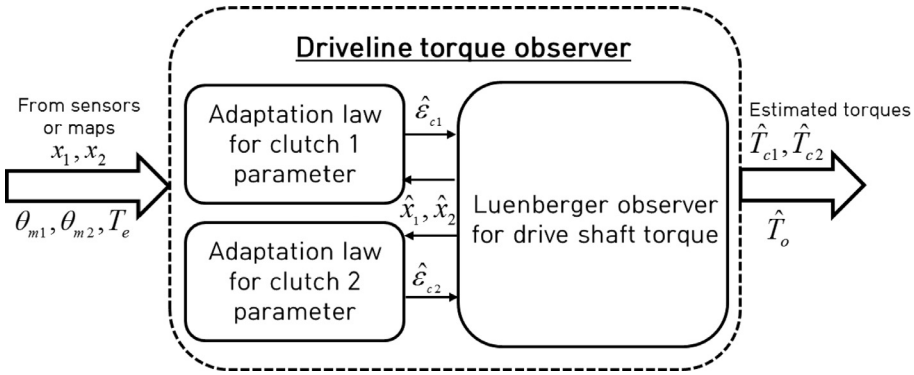

Fig. 7. Torque observer structure.

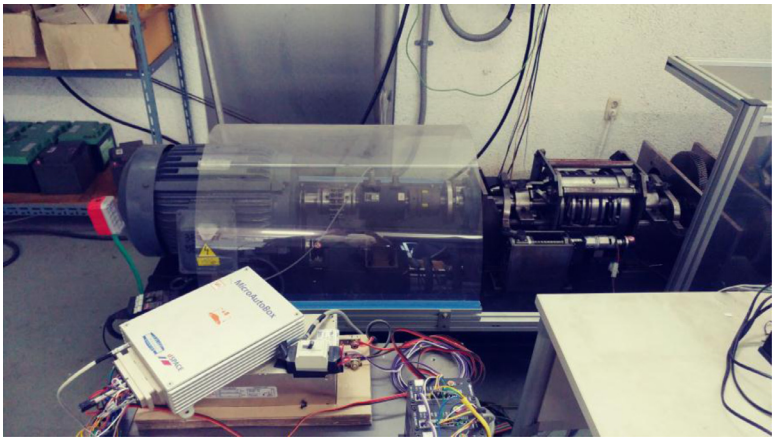

Fig. 8. Test bench set-up.

$$\begin{aligned}\dot{V} = {} & \tilde{x}_1\left(-\left(\frac{1}{J_{ed}}+\frac{i_{t2}i_{f2}}{J_{ct2,eq}}\right)r_{c2}N_2\theta_{m2}\tilde{\varepsilon}_{c2}-\left(\frac{1}{J_{ed}}+\frac{i_{t1}i_{f1}}{J_{ct2,eq}}\right)r_{c1}N_1\theta_{m1}\tilde{\varepsilon}_{c1}\right)-L_{11}\tilde{x}_1^2\\ & +\tilde{x}_2\left(\frac{i_{t1}i_{f1}}{i_{t2}i_{f2}J_{ct2,eq}}r_{c1}N_1\theta_{m1}\tilde{\varepsilon}_{c1}+\frac{1}{J_{ct2,eq}}r_{c2}N_2\theta_{m2}\tilde{\varepsilon}_{c2}\right)-L_{22}\left(c_{o,eq}^2+1\right)\tilde{x}_2^2-c_{o,eq}\left(-\frac{1}{i_{t2}i_{f2}J_{ct2,eq}}-\frac{1}{J_v}\right)\tilde{x}_2^2\\ & -\frac{1}{L_{c1}}\tilde{\varepsilon}_{c1}\dot{\hat{\varepsilon}}_{c1}-\frac{1}{L_{c2}}\tilde{\varepsilon}_{c2}\dot{\hat{\varepsilon}}_{c2}.\end{aligned} \tag{28}$$

Then, the following adaptation laws are defined to make $\dot{V}$ negative semi-definite:

$$\begin{aligned}\dot{\hat{\varepsilon}}_{c1} &\triangleq L_{c1}\left(-\left(\tfrac{1}{J_{ed}}+\tfrac{i_{t1}i_{f1}}{J_{ct2,eq}}\right)\tilde{x}_1+\tfrac{i_{t1}i_{f1}}{i_{t2}i_{f2}J_{ct2,eq}}\tilde{x}_2\right)r_{c1}N_1\theta_{m1}\\ \dot{\hat{\varepsilon}}_{c2} &\triangleq L_{c2}\left(-\left(\tfrac{1}{J_{ed}}+\tfrac{i_{t2}i_{f2}}{J_{ct2,eq}}\right)\tilde{x}_1+\tfrac{1}{J_{ct2,eq}}\tilde{x}_2\right)r_{c2}N_2\theta_{m2}.\end{aligned} \tag{29}$$

The adaptation laws, $\dot{\hat{\varepsilon}}_{c1}$and $\dot{\hat{\varepsilon}}_{c2}$ have a role to continuously correct the clutch parameter values in accordance with the errors between the observer's responses and the actual measurements, $\tilde{x}_1,\ \tilde{x}_2$. If the values of either $\tilde{x}_1,\ \tilde{x}_2$ or θ_{m1}, θ_{m2} stay near zero, then the adaptation laws also becomes zero, which indicates no further correction of the clutch parameter values.

Combining (28) with (29) leads to (30):

$$\dot{V} = -L_{11}\tilde{x}_1^2-L_{22}\left(c_{o,eq}^2+1\right)\tilde{x}_2^2+c_{o,eq}\left(\frac{1}{i_{t2}i_{f2}J_{ct2,eq}}+\frac{1}{J_v}\right)\tilde{x}_2^2\le 0. \tag{30}$$

The inequality is always valid since $L_{11}>0$ and $L_{22}>\frac{c_{o,eq}}{(c_{o,eq}^2+1)}\left(\frac{1}{i_{t2}i_{f2}J_{ct2,eq}}+\frac{1}{J_v}\right)$. From the inequality (30), it is inferred that $\dot{V}$ is negative semi-definite, and the boundedness of the estimation errors is guaranteed. Next, the following set is considered to prove the asymptotic stability of the observer:

$$\Omega = \{\ \tilde{x}_1,\ \tilde{x}_2,\ \tilde{x}_3,\ \tilde{\varepsilon}_{c1},\ \tilde{\varepsilon}_{c2}\mid \tilde{x}_1,\ \tilde{x}_2=0\}, \tag{31}$$

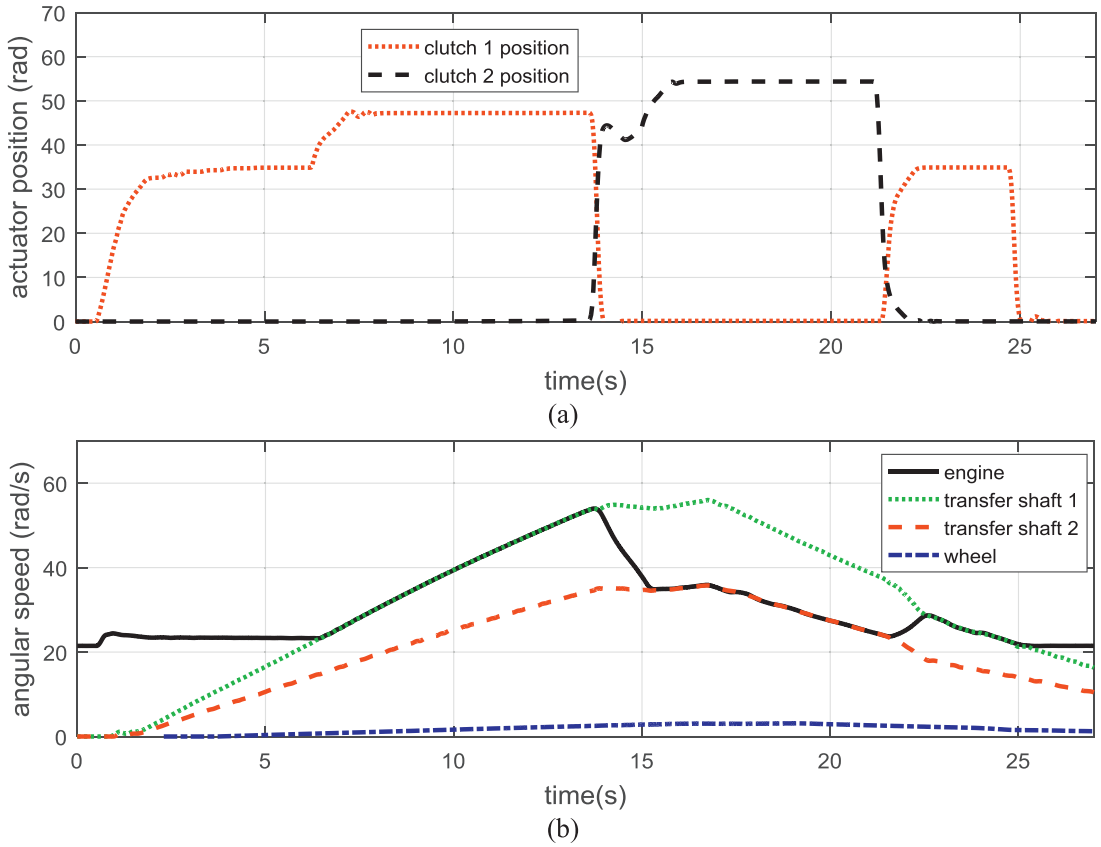

Fig. 9. Test scenario: (a) clutch actuator position, (b) driveline speed.

Table 1
Parameters for Experiments.

Parameter	Value	Parameter	Value
J_e	0.745 kg·m^2	$k_{o,\,eq}$	4887 N·m/rad
J_d	0.0165 kg·m^2	$c_{o,\,eq}$	567 N·m·s /rad
J_{ct1}	0.1 kg·m^2	i_{t1}	3
J_{ct2}	0.1 kg·m^2	i_{t2}	2.4
J_o	0.04 kg·m^2	i_{f1}	6
J_v	134.6 kg·m^2	i_{f2}	4.8
$r_{c1}N_1$	0.095 m	$r_{c2}N_2$	0.095 m

where $V = 0$. When $\tilde{x}_{3e}$ denotes the steady state value of $\tilde{x}_3$, it is deduced from (15) that in the set Ω, $\tilde{x}_{3e}$ can be represented as a summation of $\tilde{\varepsilon}_{c1}$ and $\tilde{\varepsilon}_{c2}$ multiplied by some constants, i.e., $\tilde{x}_{3e} = \alpha\tilde{\varepsilon}_{c1} + \beta\tilde{\varepsilon}_{c2}$ where α, β are the constants. Thus, $\tilde{x}_1,\ \tilde{x}_2 = 0$implies $\tilde{\varepsilon}_{c1},\ \tilde{\varepsilon}_{c2} = 0$ as well as $\tilde{x}_3 = 0$ in Ω. In other words, the origin $\tilde{x}_1 = \tilde{x}_2 = \tilde{x}_3 = \tilde{\varepsilon}_{c1} = \tilde{\varepsilon}_{c2} = 0$ is the only invariant subset of Ω that guarantees all the estimation errors are asymptotically converged to zero in a finite time [37]. The resulting torque observer performs simultaneous estimation of the state (T_o) and the unknown inputs (T_{c1}, T_{c2}), and its structure is schematically depicted in Fig. 7. Here, the developed torque observer requires the measurement of each clutch actuator position for parameter updates and not the dynamics of the actuators. In other words, the observer only uses the driveline dynamics, so it is applicable to general DCTs, regardless of the type or dynamics of the clutch actuators. In the case of the wet DCT, where the position value cannot be measured, the clutch pressure information is often available, so it can be alternatively used to derive the adaptive scheme in the same way as (29).

4. Experiments

4.1. Experimental Set-ups

Several experiments were conducted in order to demonstrate the torque observer's performance. As depicted in Fig. 8, a DCT driveline test-bench where torque sensors are mounted were used for validation. This is because the torque sensors

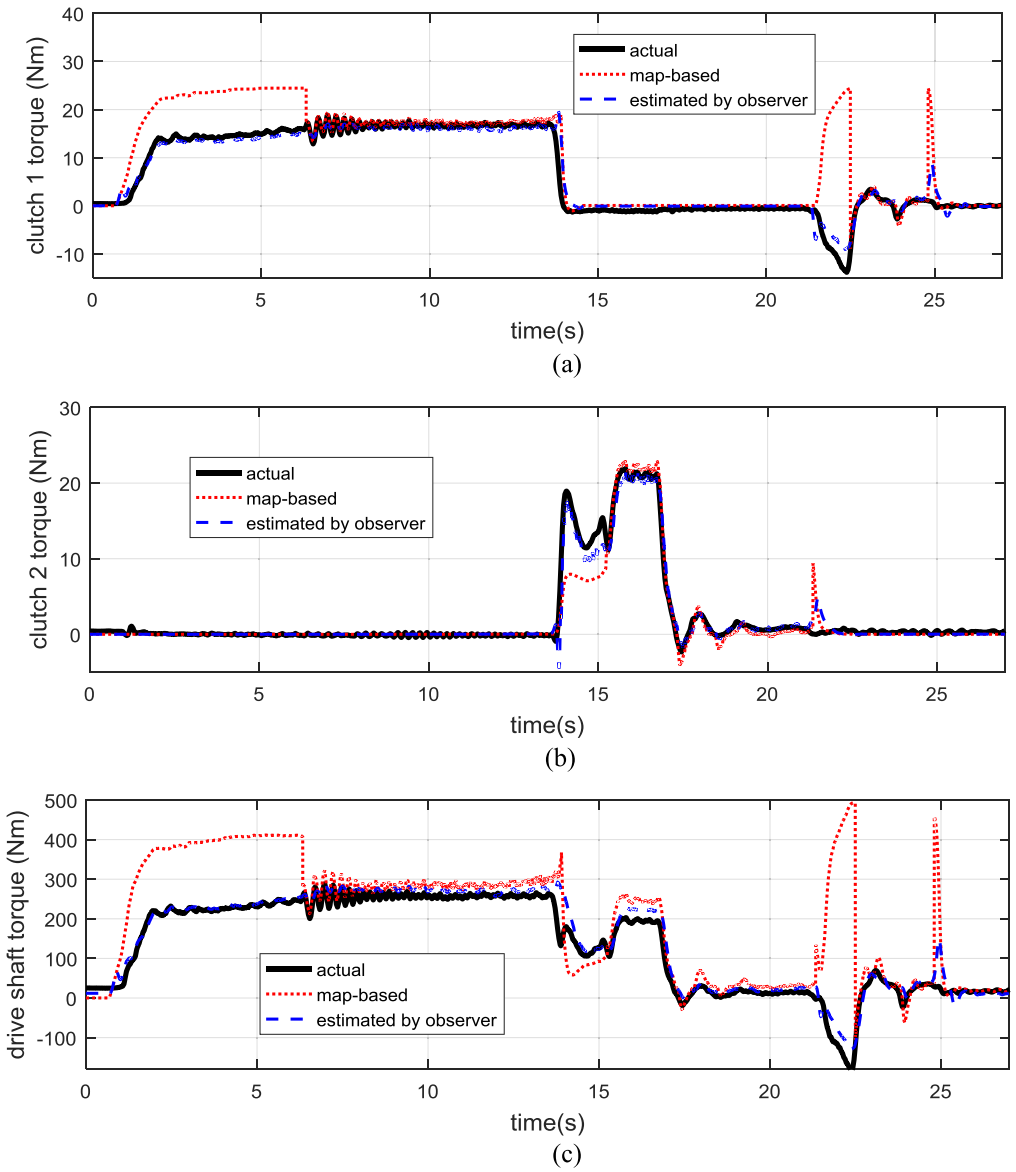

Fig. 10. Torque estimation results for case (1): (a) clutch 1 torque, (b) clutch 2 torque, (c) drive shaft torque.

cannot be installed in an actual vehicle because of spatial limitation. The parameter values identified are provided in Table 1. In the test DCT, torque transducers as well as encoders were installed on the shafts to obtain the actual torque transmitted through the driveline for validation purposes. In the experiments, MicroAutoBox dSPACE 1401 was used to run the torque observer algorithm and process the sensor signals.

The primary objective of conducting the experiments is to validate the estimation accuracy of the torque observer that covers various driving conditions and its robustness to parametric uncertainties. As described in the introductory section, the most difficult condition for estimating the driveline torque is when the vehicle performs a gear shift. During gear shifts in vehicles with a DCT, the torque through both clutches needs to be identified simultaneously for the final estimation of the drive shaft torque. Hence, a test scenario was determined such that it contained multiple gear shifts along with normal driving situations. Fig. 9 illustrates the clutch actuator positions and the vehicle states corresponding to the test scenario. In the beginning of the experiment, the vehicle launched as clutch 1 was engaged with the engine. After accelerations, an upshift from 1st to 2nd gear, and then a downshift from 2nd to 1st gear occurred sequentially. In addition, the experiments were carried out for two cases of different clutch parameter values to demonstrate the error-correction ability of the adaptation laws (29). We assumed two sets of nominal values for the dynamic friction coefficients of each case: (1) $\mu_{k1,n} = 0.4,\ \mu_{k2,n} = 0.1$ and (2) $\mu_{k1,n} = 0.1,\ \mu_{k2,n} = 0.4$, which were carelessly chosen. Here, we want to verify

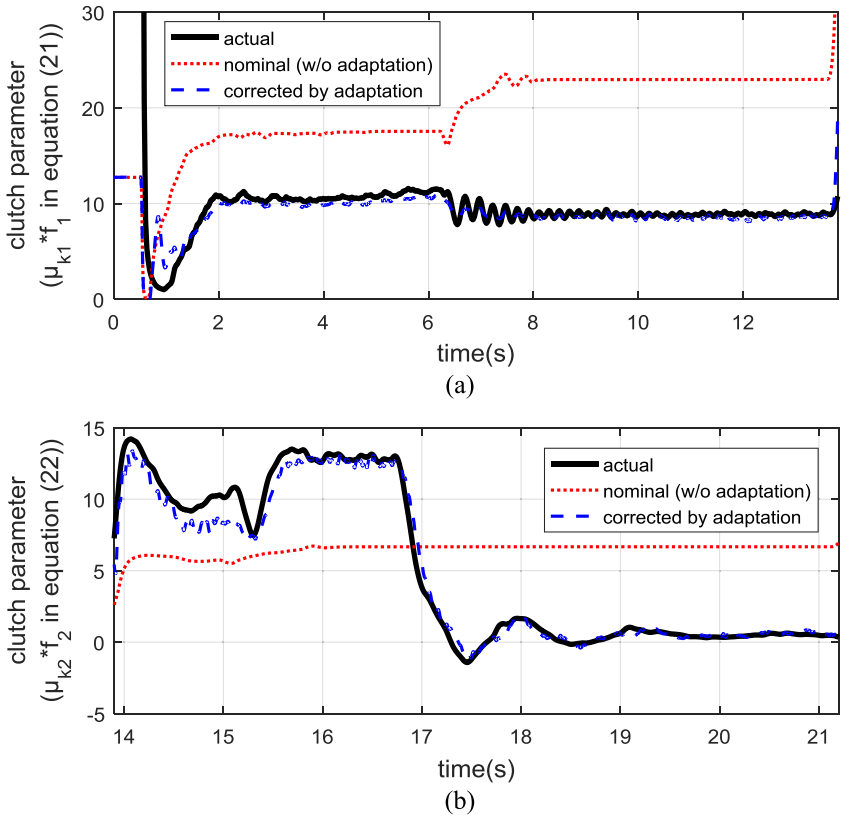

Fig. 11. Clutch parameter adaptations for case (1): (a) for clutch 1, (b) for clutch 2.

if all the estimated torques will converge near the true values in spite of the poor accuracy of the nominal parameter values.

4.2. Experimental results and discussion

4.2.1. Case (1): $\mu_{k1,n} = 0.4$, $\mu_{k2,n} = 0.1$

First, we assumed the friction coefficient values of each clutch were as follows: $\mu_{k1,n} = 0.4$ and $\mu_{k2,n} = 0.1$. The friction coefficient values could be more elaborately modeled or estimated, but such poorly chosen constants were intentionally used for a more accurate assessment of the adaptive observer's performance. Fig. 10 exhibits the corresponding test results. For the direct comparison of the proposed observer with the conventional position map-based approach, the results of map-based torque estimations merely based on the force-position map and the nominal friction coefficient were also exhibited in Fig. 10. In the map-based estimation approach, the nominal force coefficients had been acquired in advance by experiments as the look-up tables of the clutch actuator positions, and the driveline torque values were calculated using the nominal force-position maps and the nominal friction coefficients.

It was inferred from Fig. 10 that the nominal clutch parameter was significantly over-estimated for clutch 1 (Fig. 10(a)) and under-estimated for clutch 2 (Fig. 10(b)), which induced larger errors between the actual clutch torques and the map-based ones without adaptations. Thus, both the clutch torques and the drive shaft torque exhibited large estimation errors (Fig. 10(c)). It was obviously seen that the map-based approach was vulnerable to the parameter errors. On the other hand, all the torque states estimated by the proposed adaptive observer converged quickly near the true values in spite of the inaccurate nominal parameters. In the introductory section, particular emphasis was placed on the importance of the transient torque through the drive shaft in terms of shift quality. The oscillations of the drive shaft torque that occurred during the gear shifts or vehicle launch were also precisely described by the torque observer. Because the torque observer was mainly designed based on the proposed control-oriented model, it successfully captured the transient behavior of the driveline. Note that large negative torques were observed at around 22∼24 s in Figs. 10(a), (c) because the driveline was decelerated by the engine brake in this period. Though the actuator position of clutch 1 remained positive during the period so that the corresponding map-based torque was also positive, the adaptive observer still followed the actual value well by correcting the clutch parameter.

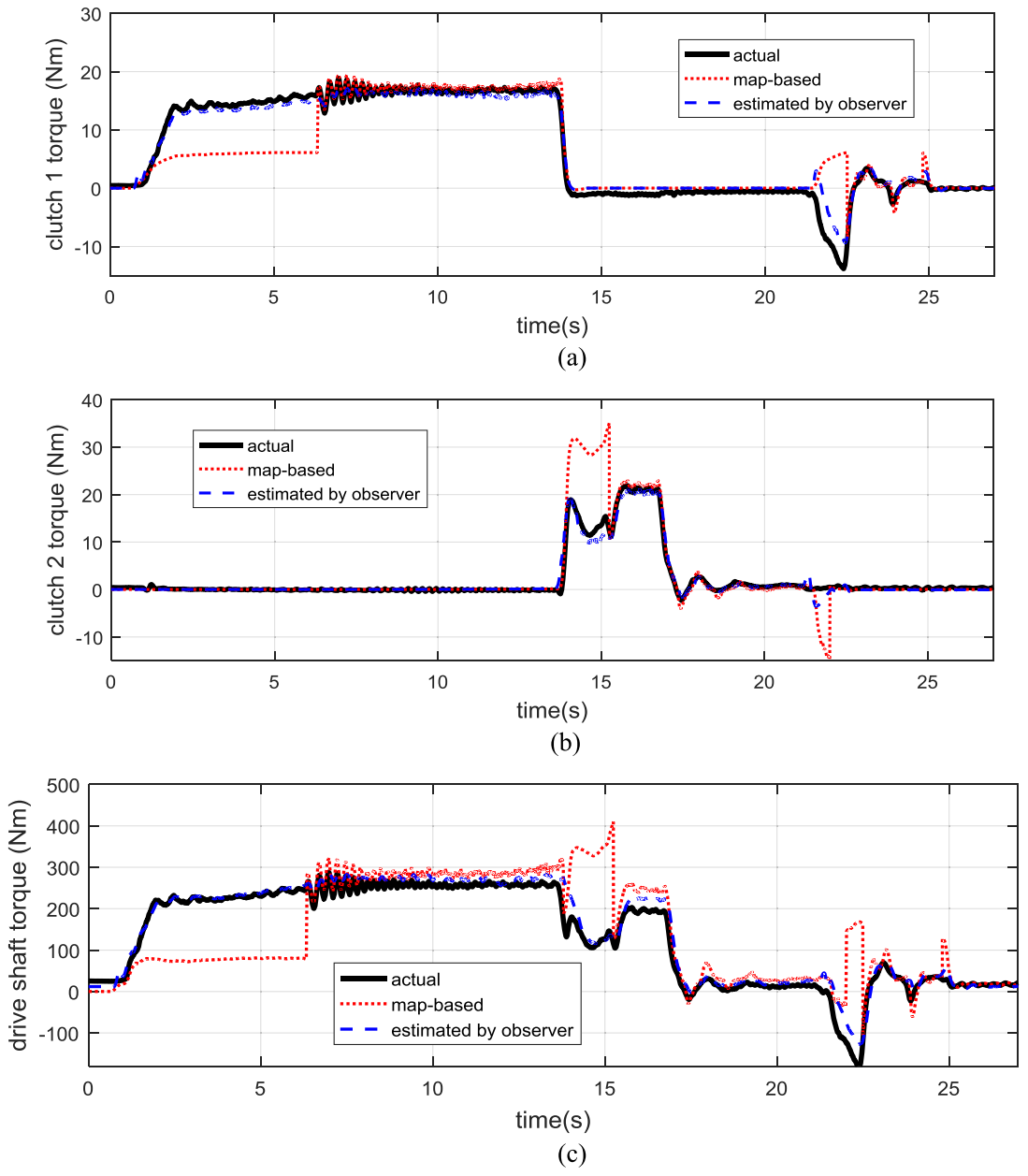

Fig. 12. Torque estimation results for case (2): (a) clutch 1 torque, (b) clutch 2 torque, (c) drive shaft torque.

In order to more clearly present how the adaptation laws (29) work during the torque estimations, plots on the variations of the clutch parameters are illustrated in Fig. 11. In Fig. 11, the y-axis denotes the variable parameters of the clutch torque model (21), (22), the dynamics friction coefficients multiplied by the coefficients of the force-position map, i.e. $\mu_{k1}f_1$, $\mu_{k2}f_2$. The large discrepancies between the nominal values and the true ones are evident in Fig. 11. It was deduced from Figs. 10,11 that torque calculations merely using the clutch actuator position information cannot cover various driving conditions because its estimation ability heavily depends on the accuracy of the nominal friction coefficient and the force-position (or torque-position) map. On the other hand, the adaptation scheme continuously corrected the parameter values from the feedback of the torque observer error, which improved the observer's performance significantly.

4.2.2. Case (2): $\mu_{k1,n} = 0.1,\ \mu_{k2,n} = 0.4$

Next, another experiment was carried out with nominal friction coefficients assigned in an opposite way to case (1). The corresponding test results are shown in Fig. 12. In this case, the map-based torque response of clutch 1 (without adaptation) exhibited large negative errors while that of clutch 2 showed positive errors, which tended to be completely opposite to

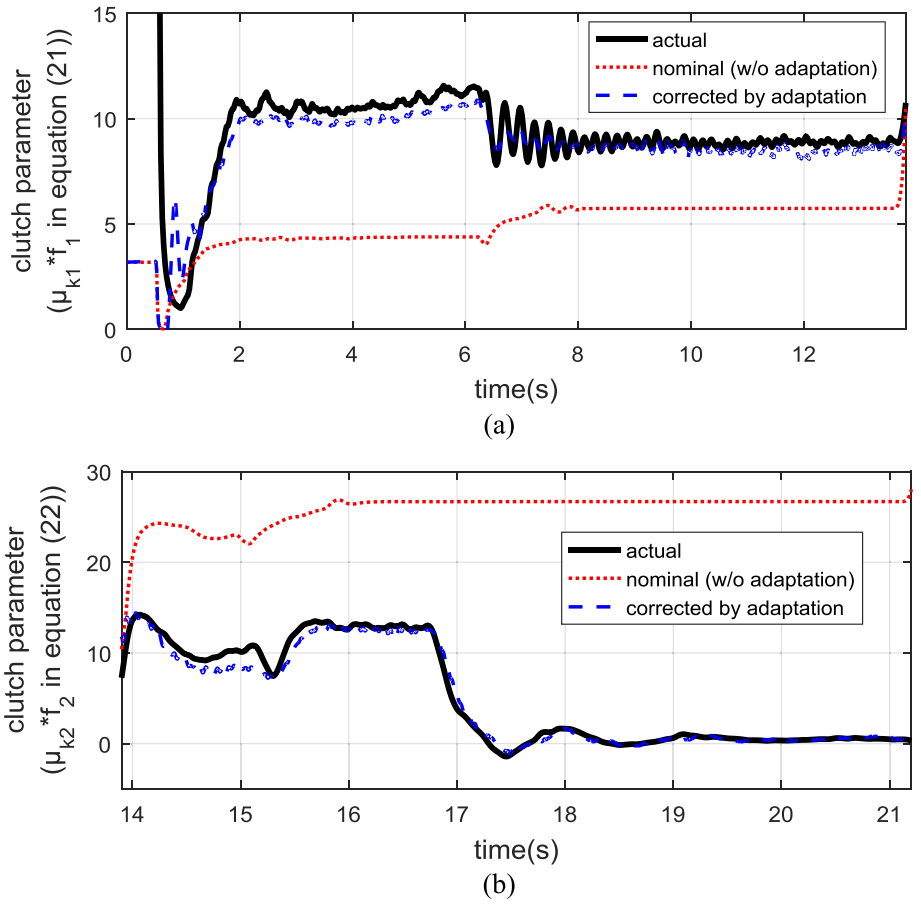

Fig. 13. Clutch parameter adaptations for case (2): (a) for clutch 1, (b) for clutch 2.

case (1). However, the torque observer still demonstrated its high estimation performance throughout the test scenario. The parameter variations of each clutch are depicted in Fig. 13, which well verified the error-correcting ability of the adaptive scheme.

It is worth noting that any structural/parametric changes or further gain tuning of the observer were not performed throughout the experiments. Nevertheless, it was demonstrated by the experiments that the proposed torque observer worked for all the general driving conditions, including the gear shifts where the two clutches were manipulated concurrently.

Another strong aspect of the torque observer is that its estimation ability is irrelevant to clutch states, i.e., whether the clutch is engaged, slipping, or disengaged. As described in (6) and (7), the clutch torque model is very different in accordance with the clutch states. Since the adaptive scheme (29) merely uses the slip torque Eqs. (21),(22), its adaptation performance may be degraded when the clutch is not slipping. However, the torque observer was designed to always meet the Lyapunov stability condition (Section 3.2). Thus, it successfully estimated the driveline torques for the given driving scenario whether the clutches are slipping or not. The test results well verified the effectiveness of the proposed torque estimation approach, which was in close agreement with the predictions from the stability proving procedure.

5. Conclusion

In a vehicle driveline with DCT, the torque delivered by the engine can flow through both clutches during shift transients, so how to control the transient torque effectively through the driveline is a key to enhance the shift quality in the absence of the dampening effects from torque converters. Thus, this study investigated the control-oriented modeling and torque estimations of the DCT driveline for practical control applications. A control-oriented driveline model was established that considered practicalities such that both the stiffness and damping characteristics of the driveline were well described without any further increments of the model order. In addition, an adaptive torque observer was developed to concurrently monitor the transmitted torque of both clutches and the drive shaft in the driveline, which can be used to significantly improve the longitudinal dynamics control quality of the vehicle as well as its powertrain control performances. The torque

observer was designed merely based on the proposed driveline dynamics, which is applicable to general DCTs, so that its estimation ability is not relevant to certain dynamics of the clutch actuators.

It was clearly observed from the experimental results on the DCT test-bench that the torque observer predicted the driveline torque states precisely in spite of the clutch parameter errors. The observer works under all normal driving conditions, including vehicle launch and gear shifts. In this study, it was assumed that all the rotational inertias in the vehicle driveline were constant during normal driving conditions. However, the lumped inertia values, particularly the vehicle inertia, can be varied according to driving circumstances. Therefore, it remains for future studies to effectively deal with such vehicle parameter uncertainties in the related works on control or state estimation of vehicle powertrains.

Acknowledgment

This work was supported by Agency for Defense Development, Korea.

References

[1] Y. Zhang, X. Chen, X. Zhang, W. Tobler, H. Jiang, Dynamic modeling of a dual-clutch automated lay-shaft transmission, in: ASME 2003 International Design Engineering Technical Conferences and Computers and Information in Engineering Conference, 2003, pp. 703–708.
[2] H.R. Lee, C.S. Kim, and T.C. Kim, “Double clutch transmission for a hybrid electric vehicle and method for operating the same,” ed: US Patent Application 7249537 B2, 2009.
[3] P.D. Walker, N. Zhang, Active damping of transient vibration in dual clutch transmission equipped powertrains: a comparison of conventional and hybrid electric vehicles, Mech. Mach. Theory 77 (2014) 1–12.
[4] X. Zhou, P. Walker, N. Zhang, B. Zhu, J. Ruan, Numerical and experimental investigation of drag torque in a two-speed dual clutch transmission, Mech. Mach. Theory 79 (2014) 46–63.
[5] Z. Lei, D. Sun, Y. Liu, D. Qin, Y. Zhang, Y. Yang, et al., Analysis and coordinated control of mode transition and shifting for a full hybrid electric vehicle based on dual clutch transmissions, Mech. Mach. Theory 114 (2017) 125–140.
[6] Z. Sun, K. Hebbale, Challenges and opportunities in automotive transmission control, in: American Control Conference, 2005. Proceedings of the 2005, 2005, pp. 3284–3289.
[7] M. Goetz, M. Levesley, D. Crolla, Dynamics and control of gearshifts on twin-clutch transmissions, in: Proceedings of the institution of mechanical engineers, Part D: Journal of Automobile Engineering, 219, 2005, pp. 951–963.
[8] M. Kulkarni, T. Shim, Y. Zhang, Shift dynamics and control of dual-clutch transmissions, Mech. Mach. Theory 42 (2007) 168–182.
[9] P.D. Walker, N. Zhang, R. Tamba, Control of gear shifts in dual clutch transmission powertrains, Mech. Syst. Signal Proc. 25 (2011) 1923–1936.
[10] K. van Berkel, T. Hofman, A. Serrarens, M. Steinbuch, Fast and smooth clutch engagement control for dual-clutch transmissions, Control Eng. Practice 22 (2014) 57–68.
[11] Y. Liu, D. Qin, H. Jiang, Y. Zhang, Shift control strategy and experimental validation for dry dual clutch transmissions, Mech. Mach. Theory 75 (2014) 41–53.
[12] S. Kim, J. Oh, S. Choi, Gear shift control of a dual-clutch transmission using optimal control allocation, Mech. Mach. Theory 113 (2017) 109–125.
[13] E. Galvagno, M. Velardocchia, A. Vigliani, Dynamic and kinematic model of a dual clutch transmission, Mech. Mach. Theory 46 (2011) 794–805.
[14] K.-s. Yi, B.-K. Shin, K.-I. Lee, Estimation of turbine torque of automatic transmissions using nonlinear observers, J. Dynamic Syst. Meas. Control 122 (2000) 276–283.
[15] J.-O. Hahn, K.-I. Lee, Nonlinear robust control of torque converter clutch slip system for passenger vehicles using advanced torque estimation algorithms, Veh. Syst. Dynamics 37 (2002) 175–192.
[16] B.K. Shin, J.O. Hahn, and K.I. Lee, "Development of shift control algorithm using estimated turbine torque," SAE Technical Paper 0148-7191, 2000.
[17] R.A. Masmoudi, J.K. Hedrick, Estimation of vehicle shaft torque using nonlinear observers, J. Dynamic Syst. Meas. Control 114 (1992) 394–400.
[18] S. Watechagit and K. Srinivasan, "Modeling and simulation of a shift hydraulic system for a stepped automatic transmission," SAE Technical Paper 0148-7191, 2003.
[19] M. Ibamoto, H. Kuroiwa, T. Minowa, K. Sato, and T. Tsuchiya, "Development of smooth shift control system with output torque estimation," SAE Technical Paper 0148-7191, 1995.
[20] B. Gao, H. Chen, Y. Ma, K. Sanada, Design of nonlinear shaft torque observer for trucks with automated manual transmission, Mechatronics 21 (2011) 1034–1042.
[21] J. Kim, S.B. Choi, Control of dry clutch engagement for vehicle launches via a shaft torque observer, in: American Control Conference (ACC), 2010, 2010, pp. 676–681.
[22] Z.-G. Zhao, J.-L. Jiang, Z.-P. Yu, T. Zhang, Starting sliding mode variable structure that coordinates the control and real-time optimization of dry dual clutch transmissions, Int. J. Automotive Technol. 14 (2013) 875–888.
[23] M. Wu, J. Zhang, T. Lu, C. Ni, Research on optimal control for dry dual-clutch engagement during launch, in: Proceedings of the Institution of Mechanical Engineers, Part D: Journal of Automobile Engineering, 224, 2010, pp. 749–763.
[24] V. Tran, J. Lauber, M. Dambrine, Sliding mode control of a dual clutch during launch, in: The second international conference on engineering mechanics and automation (ICEMA2), 2012, pp. 16–17.
[25] Z. Zhao, X. Li, L. He, C. Wu, J.K. Hedrick, Estimation of torques transmitted by twin-clutch of dry dual clutch transmission during vehicle's launching process, IEEE Trans. Veh. Technol (2016).
[26] Z. Zhao, L. He, Y. Yang, C. Wu, X. Li, J.K. Hedrick, Estimation of torque transmitted by clutch during shifting process for dry dual clutch transmission, Mech. Syst. Signal Proc. 75 (2016) 413–433.
[27] H. Hao, T. Lu, J. Zhang, Estimation of transmitted torques in dual-clutch transmission systems, Insight-Non-Destr. Test. Condition Monit. 57 (2015) 464–471.
[28] R. Losero, J. Lauber, T.-M. Guerra, P. Maurel, Dual clutch torque estimation Based on an angular discrete domain Takagi-Sugeno switched observer, in: Fuzzy Systems (FUZZ-IEEE), 2016 IEEE International Conference on, 2016, pp. 2357–2363.
[29] J.J. Oh, S.B. Choi, J. Kim, Driveline modeling and estimation of individual clutch torque during gear shifts for dual clutch transmission, Mechatronics 24 (2014) 449–463.
[30] J.J. Oh, S.B. Choi, Real-time estimation of transmitted torque on each clutch for ground vehicles with dual clutch transmission, Mechatron. IEEE/ASME Trans. 20 (2015) 24–36.
[31] M. Hoic, Z. Herold, N. Kranjcevic, J. Deur, V. Ivanovic, Experimental characterization and modeling of dry dual clutch thermal expansion effects, SAE Int. J. Passenger Cars-Mech. Syst. 6 (2013) 775–785.
[32] A. Myklebust, L. Eriksson, Modeling, observability, and estimation of thermal effects and aging on transmitted torque in a heavy duty truck with a dry clutch, IEEE/ASME Trans. Mechatron. 20 (2015) 61–72.
[33] A. Crowther, N. Zhang, D. Liu, J. Jeyakumaran, Analysis and simulation of clutch engagement judder and stick-slip in automotive powertrain systems, Proc. Inst. Mech. Eng. Part D: J. Autom. Eng. 218 (2004) 1427–1446.
[34] J. Kim, "An automotive clutch control for vibration suppression of dual clutch transmissions," SAE Technical Paper 0148-7191, 2016.

[35] X. Zhu, F. Meng, H. Zhang, Y. Cui, Robust driveshaft torque observer design for stepped ratio transmission in electric vehicles, Neurocomputing 164 (2015) 262–271.
[36] F. Vasca, L. Iannelli, A. Senatore, G. Reale, Torque transmissibility assessment for automotive dry-clutch engagement, Mechatron. IEEE/ASME Trans. 16 (2011) 564–573.
[37] P.A. Ioannou and J. Sun, *Robust adaptive control*: courier corporation, 2012.